

# Synthesis and electrical conductivity of perovskite-type $\text{PrCo}_{1-x}\text{Mg}_x\text{O}_3$

Yinzhe Ren, Baoan Li\*, Jianying Wang, Xiaohong Xu

*School of Chemistry and Materials Science, Shanxi Normal University, Linfen 041004, China*

Received 10 February 2004; received in revised form 27 May 2004; accepted 16 July 2004

Available online 6 October 2004

## Abstract

Oxides in the system  $\text{PrCo}_{1-x}\text{Mg}_x\text{O}_3$  ( $x = 0.0, 0.05, 0.10, 0.15, 0.20, 0.25$ ) were synthesized by citrate technique and characterized by powder X-ray diffraction and scanning electron microscope. All compounds have a cubic perovskite structure (space group  $O_h^1\text{-Pm}\bar{3}m$ ). The maximum ratio of doped Mg in the system  $\text{PrCo}_{1-x}\text{Mg}_x\text{O}_3$  is  $x = 0.2$ . Further doping leads to the segregation of  $\text{Pr}_6\text{O}_{11}$  in  $\text{PrCo}_{1-x}\text{Mg}_x\text{O}_3$ . The substitution of Mg for Co improves the performance of  $\text{PrCoO}_3$  as compared to the electrical conductivity measured by a four-probe electrical conductivity analyzer in the temperature range from 298 to 1073 K. The substitution of Mg for Co on the *B* site may be compensated by the formations of  $\text{Co}^{4+}$  and oxygen vacancies. The electrical conductivity of  $\text{PrCo}_{1-x}\text{Mg}_x\text{O}_3$  oxides increases with increasing  $x$  in the range of 0.0–0.2. The increase in conductivity becomes considerable at the temperatures  $\geq 673$  K especially for  $x \geq 0.1$ ; it reaches a maximum at  $x = 0.2$  and 1073 K. From  $x > 0.2$  the conductivity of  $\text{PrCo}_{1-x}\text{Mg}_x\text{O}_3$  starts getting lower. This is probably a result of the segregation of  $\text{Pr}_6\text{O}_{11}$  in  $\text{PrCo}_{1-x}\text{Mg}_x\text{O}_3$ , which blocks oxygen transport, and association of oxygen vacancies. A change in activation energy for all  $\text{PrCo}_{1-x}\text{Mg}_x\text{O}_3$  compounds ( $x = 0-0.25$ ) was observed, with a higher activation energy above 573 K and a lower activation energy below 573 K. The reasons for such a change are probably due to the change of dominant charge carriers from  $\text{Co}^{4+}$  to  $\text{V}_\text{o}$  in  $\text{PrCo}_{1-x}\text{Mg}_x\text{O}_3$  oxides and a phase transition mainly starting at 573 K.

© 2004 Elsevier Inc. All rights reserved.

**Keywords:**  $\text{PrCo}_{1-x}\text{Mg}_x\text{O}_3$ ; Perovskite; Electrical conductivity; X-ray

## 1. Introduction

$\text{PrCoO}_3$  oxide has been studied extensively as a catalyst for effluent gas treatment [1], esterification [2], methane oxidation [3], CO oxidation [4] and so on. Non-doped and doped  $\text{PrCoO}_3$  perovskite materials are receiving great attention due to their utilization in various electrochemical processes such as solid oxide fuel cells (SOFC) [5,6], membranes for oxygen separation [7] and gas sensors [8,9]. The crystal structure, thermal, electrical and magnetic properties of these

$\text{Pr}_{1-x}\text{B}_x\text{CoO}_3$  oxides ( $B^{2+} = \text{Sr}^{2+}, \text{Ba}^{2+}, \text{Ca}^{2+}, \text{Pb}^{2+}$ ) have been investigated by many researchers [10–18]. Among them,  $\text{Pr}_{1-x}\text{Sr}_x\text{CoO}_3$  oxides have been studied in the most detail because they have high electrical conductivity as well as high oxygen ion conductivity. Doping with an alkaline earth cation at the *A*-site is known to enhance the electronic and ionic conductivity as a result of the oxidation of  $\text{Co}^{3+}$  to  $\text{Co}^{4+}$  and the formation of oxygen vacancies, respectively. Yet, little published information is available regarding the oxides of the system  $\text{PrCo}_{1-x}\text{B}_x\text{O}_3$  in which doping with an alkaline earth cation occurs at the *B*-site. It is essential to study their properties before these materials are considered for use in the above-mentioned applications. In this study, a series of *B*-site doped perovskite-type  $\text{PrCo}_{1-x}\text{Mg}_x\text{O}_3$  oxides ( $x = 0.0, 0.05, 0.10, 0.15, 0.20$ ,

\*Corresponding author. Present address: Department of Chemical Engineering, New Jersey Institute of Technology, University Heights, Newark, NJ 07102, USA. Fax: +1-201-997-4366.

E-mail address: [baolanl@yahoo.ca](mailto:baolanl@yahoo.ca) (B. Li).

0.25) have been prepared using the citrate technique; their microstructures, crystal structures and electrical conductivities have been investigated using a scanning electron microscope, powder X-ray diffraction and a four-probe electrical conductivity analyzer, respectively, and the variations of electrical conductivity with  $x$  and temperature are discussed.

## 2. Experimental

High-purity precursors ( $\text{Pr}_6\text{O}_{11}$ ,  $\text{MgO}$  and  $\text{Co}(\text{NO}_3)_2 \cdot 6\text{H}_2\text{O}$ ) were used as starting materials. Before the synthesis  $\text{MgO}$  was sintered in air at 1273 K for 8 h in order to decompose  $\text{MgCO}_3$  formed due to the reaction with  $\text{CO}_2$  in air. In this typical synthesis,  $\text{Pr}_6\text{O}_{11}$  and  $\text{MgO}$  were dissolved in nitric acid, respectively, and  $\text{Co}(\text{NO}_3)_2 \cdot 6\text{H}_2\text{O}$  was dissolved in de-ionized water. The three nitrate cation solutions were mixed in a desired cation stoichiometry. Then a certain volume of mixture of citric acid and ethylene glycol was introduced drop by drop into the cation mixture as a chelating and combustion agent. The latest solution was transparent. After allowing the resulting solution to age at 298 K for 24 h, the obtained product was dried at 373 K and finally calcined in air at 1250 K for 8 h. A series of  $\text{PrCo}_{1-x}\text{Mg}_x\text{O}_3$  oxides ( $x = 0.0, 0.05, 0.10, 0.15, 0.20, 0.25$ ) were prepared by the citrate technique.

The morphology of  $\text{PrCo}_{1-x}\text{Mg}_x\text{O}_3$  powders was studied by scanning electron microscopic analysis (SEM) and its crystal structure at room temperature was determined by powder X-ray diffraction (XRD) using  $\text{CuK}\alpha$  radiation.

The electrical conductivity was determined by a self-made four-probe electrical conductivity analyzer. The powder of the perovskite oxide was flaked into a circular slice with diameter 13 mm and thickness 2 mm by applying a pressure of 12 MPa. Each surface of the circular slice, sintered at 1250 K for 2 h, was mechanically polished by plating an Au membrane as a pole, then connected to a conductivity meter by a gold wire for the measurement of conductivity. Conductivity performances of the perovskite oxides were measured between 298 and 1073 K in air.

## 3. Results and discussion

SEM analysis revealed that the  $\text{PrCo}_{1-x}\text{Mg}_x\text{O}_3$  ( $x = 0.0, 0.05, 0.10, 0.15, 0.20, 0.25$ ) powders contain approximately spherical dense particles with diameters in the range of 40–100 nm. The SEM photograph of  $\text{PrCo}_{1-x}\text{Mg}_x\text{O}_3$  ( $x = 0.2$ ) (magnified 30.0 KX) is shown in Fig. 1. Particle diameter distribution for this case is in the range of 50–90 nm. The average particle sizes

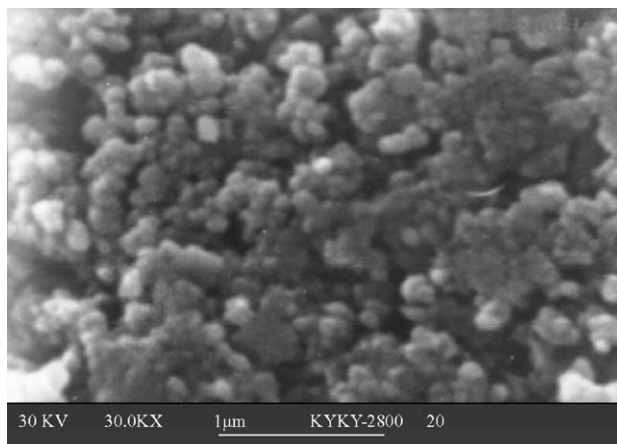


Fig. 1. SEM photograph of sample  $\text{PrCo}_{0.8}\text{Mg}_{0.2}\text{O}_3$ .

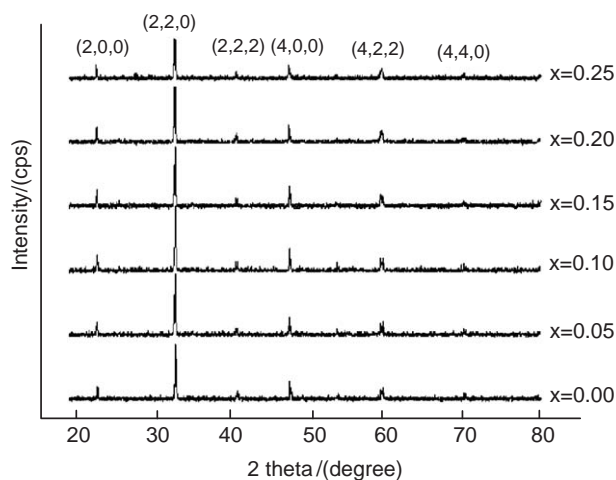


Fig. 2. XRD patterns of  $\text{PrCo}_{1-x}\text{Mg}_x\text{O}_3$  oxides.

estimated from the XRD peak widths by the Debye–Scherrer equation are also in the above range.

The crystal structure of  $\text{PrCo}_{1-x}\text{Mg}_x\text{O}_3$  samples at 298 K was measured by XRD. The XRD patterns of the compositions in the range  $0 \leq x \leq 0.25$  were indexed in the cubic perovskite structure (space group  $O_h^1-Pm\bar{3}m$ ). Typical XRD patterns are shown in Fig. 2. The diffraction peaks slightly move to a smaller angle with the increase of Mg content. That is because  $\text{Mg}^{2+}$  has a larger diameter than  $\text{Co}^{3+}$  (the diameter of hexacoordinated  $\text{Mg}^{2+}$  is 0.072 nm and that of hexacoordinated  $\text{Co}^{3+}$  is 0.0545 nm) [19]. The maximum ratio of magnesium in the system  $\text{PrCo}_{1-x}\text{Mg}_x\text{O}_3$  is  $x = 0.2$ . The further doping leads to the segregation of  $\text{Pr}_6\text{O}_{11}$  in  $\text{PrCo}_{1-x}\text{Mg}_x\text{O}_3$ . For the  $x = 0.25$  sample,  $\text{Pr}_6\text{O}_{11}$  presents in fairly low quantity at approximately  $2\theta = 28.5^\circ$ . This trend is also common for numerous other perovskite systems [20,21].

The electrical conductivity of the system  $\text{PrCo}_{1-x}\text{Mg}_x\text{O}_3$  ( $x = 0.0, 0.05, 0.10, 0.15, 0.20, 0.25$ ) for the experimental temperature range is shown in Fig. 3. All

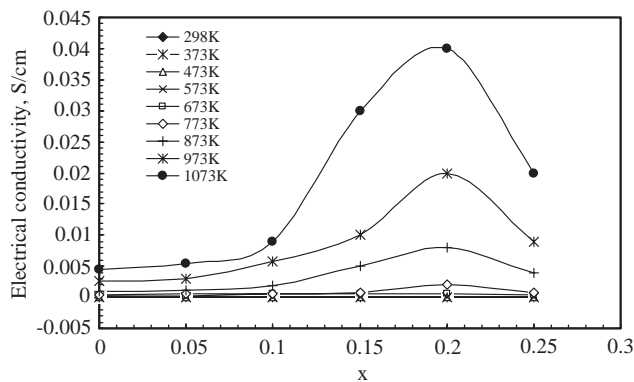
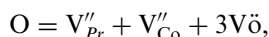


Fig. 3. Electrical conductivity of  $\text{PrCo}_{1-x}\text{Mg}_x\text{O}_3$  oxides at various temperatures as a function of  $x$ .

samples with  $x > 0$  exhibited higher electrical conductivity than the sample with  $x = 0$ . This suggests that the substitution of Mg for Co on the B site improves the performance of  $\text{PrCoO}_3$  as compared to the electrical conductivity which increases with an increase in  $x$  in the range of 0.0–0.2, and reaches a maximum at  $x = 0.2$ . This variation of electrical conductivity with the  $x$  value can be explained due to the formation of  $\text{Co}^{4+}$  and oxygen vacancies in order to compensate Mg charge. For the non-doped and slightly doped samples, the formation of  $\text{Co}^{4+}$  is favored at a low temperature [13]. The resource of oxygen vacancy is mostly from hot flaw and the concentration of oxygen vacancy is very low and temperature dependent. Oxygen vacancy ( $\text{V}_\text{O}$ ) must satisfy the following redox equilibrium:



$$K_1 = [\text{V}''_{\text{Pr}}][\text{V}''_{\text{Co}}][\text{V}_\text{O}]^3,$$

where the Kröger–Vink notation is adopted [22].

The relative importance of oxygen deficiency is increased with increasing  $\text{Mg}^{2+}$  content and temperature. The formation of oxygen vacancies can be presented as



With moderate amounts of cobalt substituted with magnesium, great numbers of oxygen vacancies and  $\text{Co}^{4+}$  generate in these solids, which lead to a great electrical conductivity. At 1073 K,  $\text{PrCo}_{0.8}\text{Mg}_{0.2}\text{O}_3$  displays a maximum conductivity (0.04 S/cm) of the system  $\text{PrCo}_{1-x}\text{Mg}_x\text{O}_3$ . That is close to the value of  $\text{PrGa}_{0.8}\text{Mg}_{0.2}\text{O}_3$  (0.05 S/cm at 1173 K) [22]. The conductivity of  $\text{PrCo}_{1-x}\text{Mg}_x\text{O}_3$  starts getting lower with an increase of  $x$  when  $x > 0.2$ . This is probably a result of  $\text{Pr}_6\text{O}_{11}$  segregation in  $\text{PrCo}_{1-x}\text{Mg}_x\text{O}_3$  blocking oxygen transport. An additional reason for the reduced conductivity is probably due to oxygen vacancies ( $\text{V}_\text{O}$ ) compounding with doped atoms  $\text{Mg}'_{\text{Co}}$  into the pairs of complex atoms ( $\text{Mg}'_{\text{Co}}\text{V}_\text{O}\text{Mg}'_{\text{Co}}$ ) when  $x > 0.2$ , which leads to lower concentration of free oxygen vacancy and therefore

lower electrical conductivity. This phenomenon is also commented in the studies of similar perovskite-type oxides [13,20,23].

From the experimental data (Fig. 3), these materials show very low conductivity at temperatures below 673 K. The conductivity somewhat increases as the content of doped Mg and temperature increase. This behavior can be described by the small polaron hopping conductivity model. The charge carriers are holes ( $\text{Co}^{4+}$ ) formed electronically to compensate the substitution of  $\text{Mg}^{2+}$  for  $\text{Co}^{3+}$ . These holes jump from site to site if sufficient activation energy is acquired by the charge carrier for the transfer. The temperature dependence of electrical conductivity is presented as

$$\sigma = \frac{A}{T} \exp\left(-\frac{E}{kT}\right),$$

where  $E$  is the activation energy for hopping,  $k$  is the Boltzmann constant,  $T$  is the temperature and  $A$  is the pre-exponential factor. It is demonstrated that the concentration of oxygen vacancy and the oxygen vacancy diffusion coefficient increase with increasing temperature at the expense of  $\text{Co}^{4+}$  [13,24–27]. Therefore, it is understandable that the conductivity of  $\text{PrCo}_{1-x}\text{Mg}_x\text{O}_3$  oxides significantly increases with increasing temperature and Mg content when the temperatures are  $\geq 673$  K especially for  $x \geq 0.1$ .

A change in activation energy for all  $\text{PrCo}_{1-x}\text{Mg}_x\text{O}_3$  compounds ( $x = 0–0.25$ ) is observed in Fig. 4, with a higher activation energy above 573 K and a lower activation energy below 573 K. Similarly, activation energy changes with temperature are reported in many publications with regard to the study of different solid oxides, such as  $\text{Nd}_{1-x}\text{Sr}_x\text{FeO}_{3-\delta}$  [26],  $\text{YMnO}_3$  [28],  $\text{PrMnO}_3$  [29],  $\text{Pr}_{1-x}\text{Sr}_x\text{CoO}_{3-\delta}$  [13],  $8\text{Dy}4\text{WSB}$  [30],  $\text{LaCoO}_{3-\delta}$  [24],  $\text{PrGa}_{1-x}\text{Mg}_x\text{O}_3$  [22] and so on. The reasons for such changes are due to the change of conduction mechanism, a breakthrough at threshold value, a phase transition or thermal expansion. One can notice that the activation energy changes for electrical

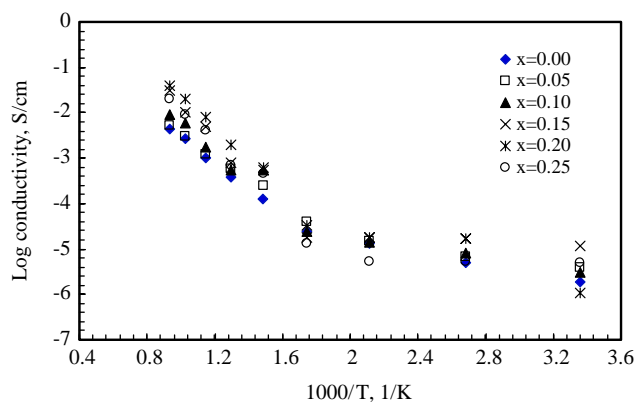


Fig. 4. Arrhenius plots of electrical conductivities for  $\text{PrCo}_{1-x}\text{Mg}_x\text{O}_3$  oxides.

conduction for the oxides as mentioned above are with a higher activation energy at lower temperatures and a lower activation energy at higher temperatures; but for the  $\text{PrCo}_{1-x}\text{Mg}_x\text{O}_3$  oxides prepared in this study the activation energy changes are reversed. The possible reasons are due to the change of dominant charge carriers from  $\text{Co}^{4+}$  to  $\text{V}_\text{o}$  in  $\text{PrCo}_{1-x}\text{Mg}_x\text{O}_3$  oxides and a phase transition mainly starting at 573 K. However, the exact nature of these changes remains unclear.

#### 4. Conclusions

Oxides in the system  $\text{PrCo}_{1-x}\text{Mg}_x\text{O}_3$  with  $x = 0.0, 0.05, 0.10, 0.15, 0.20$  and  $0.25$  were synthesized and all found to have a cubic perovskite structure (space group  $O_h^1\text{-Pm}\bar{3}m$ ). The powders contain almost spherical dense particles with diameters in the range of 40–100 nm. The maximum ratio of doped Mg in the system  $\text{PrCo}_{1-x}\text{Mg}_x\text{O}_3$  is  $x = 0.2$ . Further doping leads to the segregation of  $\text{Pr}_6\text{O}_{11}$  in  $\text{PrCo}_{1-x}\text{Mg}_x\text{O}_3$ . The substitution of Mg for Co improves the performance of  $\text{PrCoO}_3$  as compared to the electrical conductivity which increases with an increase of  $x$  in the range of 0.0–0.2. The substitution of Mg for Co on the B site may be compensated by the formations of  $\text{Co}^{4+}$  and oxygen vacancies. The formation of  $\text{Co}^{4+}$  prevails at low temperatures. Oxygen vacancies are produced as  $x$  increases and at high temperatures; its relative importance is also increased with increasing temperature and  $\text{Mg}^{2+}$  content, and above the critical values of  $x$  ( $x = 0.1$ ) and temperature ( $T = 673$  K) the formation of  $\text{V}_\text{o}$  becomes predominant. Thus, the electrical conductivity of  $\text{PrCo}_{1-x}\text{Mg}_x\text{O}_3$  oxides exhibits a significant increase with increasing temperature and Mg content with temperatures  $\geq 673$  K especially for  $x \geq 0.1$ . At 1073 K,  $\text{PrCo}_{0.8}\text{Mg}_{0.2}\text{O}_3$  displays the maximum conductivity among the studied oxides. From  $x > 0.2$  the conductivity of  $\text{PrCo}_{1-x}\text{Mg}_x\text{O}_3$  starts getting lower with an increase of  $x$  value. This is probably a result of the  $\text{Pr}_6\text{O}_{11}$  segregation in  $\text{PrCo}_{1-x}\text{Mg}_x\text{O}_3$  blocking oxygen transport and the association of oxygen vacancies. A change in activation energy for all  $\text{PrCo}_{1-x}\text{Mg}_x\text{O}_3$  compounds ( $x = 0\text{--}0.25$ ) was observed, with a higher activation energy above 573 K and a lower activation energy below 573 K. The reasons for such a change are probably due to the change of dominant charge carriers from  $\text{Co}^{4+}$  to  $\text{V}_\text{o}$  in  $\text{PrCo}_{1-x}\text{Mg}_x\text{O}_3$  oxides and a phase transition mainly starting at 573 K.

#### Acknowledgments

The authors gratefully acknowledge financial support by the Shanxi Natural Science Foundation for Basic Research (20031020) (China).

#### References

- [1] M.S. Mansinh, M. Sudhanshu, R.P. Kumar, US Patent US 6471925 (Oct. 29, 2002).
- [2] S. Sugunan, V. Meera, *React. Kinet. Catal. Lett.* 62 (2) (1997) 327.
- [3] A. Baiker, P.E. Marti, P. Keusch, E. Fritsch, A. Reller, *J. Catal.* 146 (1) (1994) 268.
- [4] Y. Chen, F. Ma, H. Lou, *Cuihua Xuebao* 7 (4) (1986) 392.
- [5] S. A. Wallin, S. D. Wijeyesekera, US Patent US 6117582 (Sep. 12, 2000).
- [6] S.A. Wallin, S.D. Wijeyesekera, Germany Patent DE 19814174 (Nov. 5, 1998).
- [7] V.V. Kharton, E.N. Naumovich, A.A. Vecher, A.V. Nikolaev, *J. Solid State Chem.* 120 (1) (1995) 128.
- [8] Y. Chen, F. Ma, H. Lou, *Hangzhou Daxue Xuebao, Ziran Kexueban* 14 (2) (1987) 189.
- [9] Kokai Tokkyo Koho, Japan Patent JP 58030648 (Feb. 23, 1983).
- [10] B. Rivas-Murias, M. Sanchez-Andujar, J. Rivas, A. Fondado, J. Mira, M.A. Senaris-Rodriguez, *NATO Science Series, II: Mathematics, Physics and Chemistry* vol. 61, 2002, p. 577.
- [11] K. Yoshii, S. Tsutsui, A. Nakamura, *J. Magn. Mater.* 226–230(Pt. 1) (2001) 829–830.
- [12] P. Shuk, V. Charton, V. Samochval, *Mater. Sci. Forum* 76(Syst. Fast Ionic Transp.) (1991) 161.
- [13] G.Ch. Kostogloudis, N. Vasilakos, Ch. Ftikos, *Solid State Ionics* 106 (1998) 207.
- [14] V.V. Kharton, A.K. Demin, *Neorg. Mater.* 29 (2) (1993) 278.
- [15] V.V. Kharton, E.N. Naumovich, A.V. Nikolaev, *J. Membr. Sci.* 111 (2) (1996) 149.
- [16] V.V. Kharton, E.N. Naumovich, A.V. Nikolaev, V.V. Samokhval, *High temperature electrochemistry: ceramics and metals, Proceedings of the 17th Risoe International Symposium on Materials Science, Roskilde, Den., September 2–6, 1996*, pp. 301–306.
- [17] H.W. Brinks, H. Fjellvaag, A. Kjekshus, B.C. Hauback, *J. Solid State Chem.* 147 (2) (1999) 464.
- [18] K. Yoshii, A. Nakamura, *Physica B: Condens. Matter (Amsterdam)* 281&282 (2000) 514.
- [19] Y. Yin, *University Chemistry Handbook, Shandong Province Science and Technologic Publishing Company, China*, 1985, pp. 1092–1093.
- [20] V.V. Kharton, A.L. Shaulo, A.P. Viskup, M. Avdeev, *Solid State Ionics* 150 (2002) 229.
- [21] V.V. Kharton, A.A. Yaremchenko, E.N. Naumovich, *J. Solid State Electrochem.* 3 (1999) 303.
- [22] Z. Liu, X. Huang, W. Liu, *Chem. J. Chin. Univ.* 22 (8) (2001) 1283.
- [23] W. Liu, K. Cheng, G. Zhang, *Chem. J. Chin. Univ.* 21 (9) (2000) 1335.
- [24] V.V. Kharton, E.N. Naumovich, A.V. Kovalevsky, A.P. Viskup, F.M. Figueiredo, I.A. Bashmakov, F.M.B. Marques, *Solid State Ionics* 138 (2000) 135.
- [25] Takamasa Ishigaki, Shigeru Yamauchi, Kohji Kishio, Junihiro Mizusaki, Kazuo Fueki, *J. Solid State Chem.* 73 (1988) 179.
- [26] N. Dasgupta, R. Krishnamoorthy, K. Thomas Jacob, *Solid State Ionics* 149 (2002) 227.
- [27] B.C.H. Steele, *Mater. Sci. Eng. B* 13 (1992) 79.
- [28] G.V.S. Subbarao, B.M. Warklyn, C.N.R. Rao, *J. Phys. Chem. Solids* 32 (1971) 345.
- [29] G.Ch. Kostogloudis, N. Vasilakos, Ch. Ftikos, *J. Eur. Ceram. Soc.* 17 (1997) 1513.
- [30] Naixiang Jiang, Eric D. Wachsman, Su-Ho. Jiang, *Solid State Ionics* 150 (2002) 347.